frontiers | Frontiers in Earth Science

TYPE Brief Research Report
PUBLISHED 02 November 2023
DOI 10.3389/feart.2023.1286817

OPEN ACCESS

EDITED BY
Paolo Capuano,
University of Salerno, Italy

REVIEWED BY
Simona Gabrielli,
National Institute of Geophysics and Volcanology (INGV), Italy
Boyko Ranguelov,
University of Mining and Geology "Saint Ivan Rilski", Bulgaria

*CORRESPONDENCE
Lisa Pierotti,
l.pierotti@igg.cnr.it

RECEIVED 31 August 2023
ACCEPTED 12 October 2023
PUBLISHED 02 November 2023

CITATION
Martinelli G, Pierotti L, Facca G and Gherardi F (2023), Geofluids as a possible unconventional tool for seismic hazard assessment.
Front. Earth Sci. 11:1286817.
doi: 10.3389/feart.2023.1286817

Geofluids as a possible unconventional tool for seismic hazard assessment

Giovanni Martinelli[1,2,3], Lisa Pierotti[4]*, Gianluca Facca[4] and Fabrizio Gherardi[4]

[1]Istituto Nazionale di Geofisica e Vulcanologia (INGV), Palermo, Italy, [2]Institute of Eco-Environment and Resources, Chinese Academy of Sciences (CAS), Lanzhou, China, [3]Laboratory of Petroleum Resources Research, Institute of Geology and Geophysics, Chinese Academy of Sciences (CAS), Lanzhou, China, [4]Consiglio Nazionale Delle Ricerche (CNR), Istituto di Geoscienze e Georisorse (IGG), Pisa, Italy

In recent decades, phenomenological methods known as Recognition of Earthquake-Prone Areas (REPA) were set up for identifying potential sites of powerful earthquakes. The information on potential earthquake sources provided by the REPA method is an essential part of seismic hazard assessment methodology. For the first time, we have combined global-scale information on the geographic occurrence of geofluids with global-scale information on earthquake occurrence, heat flow distribution, and S-wave dispersion, to gain insights into the evolution of local stress-strain fields. We focused on areas characterized by the occurrence of thermal waters and/or by the release of deep-seated gases, as traced by the isotope composition of associated helium. We noticed that the geographic distribution of these geofluids could serve as an indirect indicator of crustal permeability anomalies generated by crustal deformation procedures. This study proposes adding geofluids to the list of fundamental geological parameters to be considered in hazard assessment research.

KEYWORDS

seismic hazard, thermal waters, helium isotopes, heat flow distribution, S-wave dispersion

1 Introduction

The development of a culture of preventative measures including seismic hazard assessment, micro zonation studies, and proper building rules, can reduce the severity of the damage caused by earthquakes. In this framework, the Probabilistic Seismic Hazard Assessment (PSHA) approach has become the most prevalent and standard method for addressing seismic hazard assessment (e.g., Giardini et al., 2003). The PSHA is based on the use of probability distributions for magnitudes and source site distances recorded in earthquake catalogs, as originally proposed by Cornell (1968). The most relevant weakness of the PSHA is the dependence of the probability theory on the Gutenberg-Richter magnitude and on the completeness of available earthquake catalogs (e.g., Krinitzsky, 1995). Petersen et al. (2014) proposed to improve the PSHA by incorporating GPS and further geodetic data. Furthermore, various countries with consistent gaps in their earthquake catalogs have adopted Deterministic Seismic Hazard Assessment (DSHA) techniques (e.g., Kramer, 1996). An accurate definition of earthquake sources plays a prominent role in developing a seismic hazard assessment strategy, regardless of the applied methodology, either probabilistic or deterministic. To this purpose, a phenomenological approach for identifying possible locations of strong earthquakes was

established, known as the Recognition of Earthquake-Prone Areas (REPA) method (Gelfand et al., 1976 and references therein). The information on potential earthquake sources delivered by the REPA is an important component of the seismic hazard assessment, as envisioned by the more recent neo-deterministic seismic hazard assessment (NDSHA) methodology (Panza et al., 2012; and references therein). It combines a morpho-structural zoning method, which defines the locations of nodes over the study region, and a pattern recognition technique, which divides all the nodes into seismogenic and non-seismogenic ones to a specific cutoff of magnitude (Zhang et al., 2021; and references therein). The approach assumes that strong earthquakes are correlated with the nodes formed around intersections of lineaments. The nodes are delineated by the morpho-structural zoning method (MSZ), which is based on geomorphologic and geological data and does not rely on a knowledge of past seismicity (Gorshkov et al., 2003; Gorshkov and Soloviev, 2021). The seismogenic nodes defined by pattern recognition provide first-order systematic information that may significantly contribute to a reliable seismic hazard assessment. The information on the possible locations of strong earthquakes provided by the methodology can be directly incorporated into the neo-deterministic procedure (NDSHA) for seismic hazard assessment, filling in possible gaps in known seismicity (Panza et al., 2012). One of the main advantages of the MSZ is that it does not require prior knowledge of the regional seismicity of the studied region since it is based on the analysis of the available topographic, tectonic, and geological data, whereas paleoseismological studies require information about past seismic activity. Newer applications named Neo-Deterministic Seismic Hazard Assessment (NDSHA) proposed by Zhang et al. (2021) also take into account morpho-structural zoning, which in turn takes into account nodes (fractured areas), lineaments, and topographical features, such as the highest and lowest elevations of the studied area. The steepness of topographic surfaces and the sharpness of morphostructural parameter fluctuations, among other parameters, may indicate high tectonic activity. This paper underlines that the location of deep-seated geofluids' natural emissions is globally tied to different classes of tectonic activity because these features bring information on processes that largely occur in the lower crust. This in turn allows for identifying the surface projection of normally hidden discontinuities that influence geometry and patterns of seismic release. Thus, the geographic distribution of geofluids could be utilized as an indirect indicator of different classes of crustal permeability anomalies eventually generated by crustal deformation processes (e.g., Tamburello et al., 2018; Tamburello et al., 2022 and references therein). Moving on these grounds, this work aims to identify possible interrelations between areas of active seismicity, the location of thermal springs, and mantle-derived fluid emissions, as revealed by their $^3He/^4He$ signature, and additional geophysical parameters, such as heat flow, and S-wave distribution, in order to identify general criteria to relate seismic events and deep-seated geofluids.

2 Material and methods

We exploited the concept widely consolidated in the literature that fluid dynamics and rock deformation processes are strongly linked, to search for possible global correlations between seismicity, and a number of geophysical and geochemical parameters measurable at/from the surface. The justification for this approach stems from the fact that several authors have already highlighted a correlation between the occurrence of significant earthquakes and anomalous fluids (Irwin and Barnes, 1980; Gold and Soter, 1984; Manga et al., 2012; Chiodini et al., 2020). It is well-established that earthquakes have the potential to favor the onset of new, underground fluid flow regimes when they are capable of causing significant shaking and permanent strains in large rock volumes. Significant volumes of fluids can be permanently displaced when rocks, even with reduced initial permeability, are pervasively fractured by the upward propagation of seismogenic faults. Suitable conditions for the expulsion of thermal waters can be achieved along seismogenic faults (Curewitz and Karson, 1997; Vannoli et al., 2021; Wu et al., 2023). Geofluids can be displaced over large distances and for long times, possibly until the surface, through zones of enhanced permeability in the Earth's crust, under the effect of pressure gradients (Gleeson and Ingebritsen, 2017). Heat generation, crustal deformation, gravity effects due to the topographic relief, diagenetic processes, and overpressuring due to circulating fluids are effective mechanisms generating fundamental pressure forces at mid-crustal depth, up to the Earth's surface (Bredehoeft and Norton, 1990). On these grounds, we tried to match the information contained in a number of global, georeferenced compilations now available in the literature, to highlight possible relationships between different parameters and seismicity. In particular, we considered the following datasets: i) carbon dioxide emissions (Irwin and Barnes, 1980; Tamburello et al., 2018); ii) heat flow (Lucazeau, 2019); iii) S-wave dispersion (Debayle et al., 2016; Hasterok et al., 2022) and we updated datasets of thermal springs (Waring, 1965; Tamburello et al., 2022) and isotope composition of helium (Abedini et al., 2006). By taking advantage of recently computerized catalogs of seismicity (Storchak et al., 2013), we followed the same approach already utilized in the literature about the investigation of the spatial relationships between the distribution of earthquakes (Figure 1), and the location of anomalous fluid emissions (e.g., Kuz'mina and Novopashina, 2018; Tamburello et at., 2018), to identify areas potentially capable of hosting future strong earthquakes (M>6). A specific advancement of this work was the critical re-evaluation of the helium database by Abedini et al. (2006), and its extension via the addition of present-day geofluids data published until 2022. The largest volcanic calderas on Earth commonly extend over areas of 10–500 km^2 (Mason et al., 2004). These areas are characterized by gaseous emissions of predominant volcanic origin that are not of interest to the present treatment. Therefore, in order to filter out purely volcanic gases from our database, we decided to consider only gas emissions located beyond a prudential radius of 30 km from the main volcanic edifices worldwide.

2.1 World thermal springs dataset

In 1965, Waring compiled one of the most comprehensive available data sets about the distribution of thermal springs worldwide (Waring, 1965). More than 6,000 sites, with one or more springs for each site, were identified in more than 100 countries. Tamburello et al. (2022) digitized and enlarged

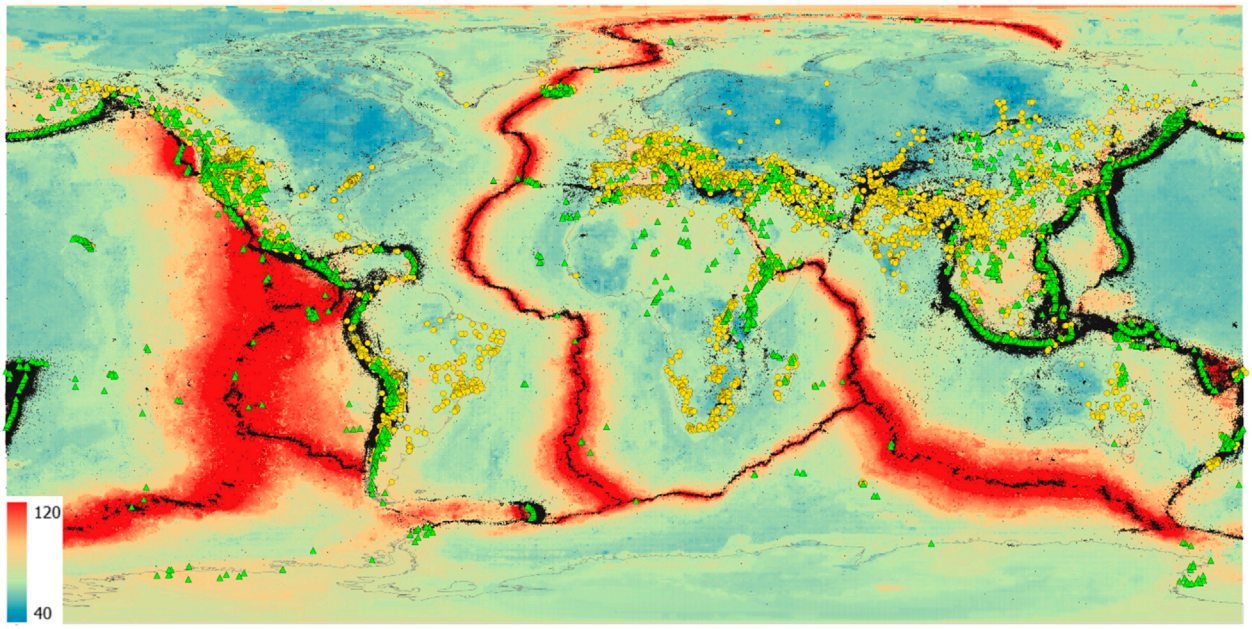

FIGURE 1
Heat flow map (Lucazeau, 2019) with location of (1) thermal springs (yellow dots; after Waring, 1965; Wexsteen, et al., 1988; Ciezkowski et al., 1992; Pesce, 2005; Wang, 2008; Lahsen et al., 2010; Yousefi et al., 2010; Chandrasekharam et al., 2015), (2) Holocenic and Pleistocenic volcanoes (green triangles; Global Volcanism Program, 2013), (3) 4<M<9.2 earthquakes (black dots; Storchak et al., 2013; http://www.isc.ac.uk/iscgem/accessed on 20 July 2023).

this data set with Supplementary Data S1 from recent literature, including additional information on geographical coordinates, temperatures, and flow rates. These data have been statistically processed and visualized with machine-learning algorithms, in a GIS environment (Graser, 2013). In order to integrate the dataset with further thermal springs in areas where possible lack of recent data was qualitatively observed such as Argentina (Pesce, 2005), Chile (Lahsen et al., 2010), China (Wang, 2008), Iran (Yousefi et al., 2010) Poland (Ciezkowski et al., 1992), Switzerland (Wexsteen, et al., 1988) and Yemen (Chandrasekharam et al., 2015), their geographic location having been georeferenced using the QGIS software (http://www.qgis.org).

2.2 World helium dataset

Helium (hereafter He) is the lightest of the noble gases, and because of its low atomic mass, is affected by strong fugacity values. He exists on Earth as two isotopes, ^3He and ^4He, with the former being primarily primordial and stored in the mantle and the latter being continuously produced in the Earth's interior by Uranium and Thorium decay (Ozima and Podosek, 2004). The radiogenic ^4He produced in the crust dominates the He flux in stable continental regions (mantle He 1%). The primordial ^3He, on the other hand, escapes into the atmosphere primarily from volcanoes and active tectonic regions (from extensive to compressive), making the He isotopic ratio ($^3He/^4He$) a powerful tool for recognizing mantle-crust tectonics also in the absence of volcanic evidence (e.g., O'nions and Oxburgh, 1983; Lupton, 1983). We consider the database compiled by Abedini et al. (2006) as a background document. In its original version (Version 1.0), this database was an MS Excel file with more than 5,000 entries on noble gas concentrations and isotopic ratios published until 2003. Data refer to geofluids and rocks from different geological and geotectonic environments. In this work, we only focus on present-day fluids discharged from springs, wells, mofetes, and fumaroles, and we complemented the dataset with additional $^3He/^4He$ analyses on geofluids published until 2022. Criteria for the selection of new data include the availability of full geographical coordinates, and/or sufficiently accurate location maps in the original manuscripts, to extract approximate information at least on the coordinates of the sampling points.

3 Discussion

3.1 Thermal springs, geodynamic and seismicity

Most of the areas hosting thermal springs overlap earthquake distribution and/or are located frequently within a radius of 30 Km from the main volcanic edifices. Further thermal springs are located outside volcanic areas in faulted zones (Figure 1).

About 60% of hydrothermal fluids recorded in the world are in the range 30°C–70°C, corresponding to the reservoir's depths in the range of 2–3 km, depending on local/regional geothermal gradients, and on the specific geometry and recharge mechanisms of the underground circulation paths. Below this range of depths, the weight of the overlying rocks significantly decreases porosity and permeability, hindering the onset of well-extended, and spatially

continuous hydrothermal circuits (Twiss and Moores, 1997). A broad literature also confirmed that vertical permeability may significantly change under the effect of tectonic activity (e.g., among many others, Wang et al., 2016; Brogi et al., 2021): faulting induced by seismic events has been effective in generating thermal springs emissions belonging to hydrothermal systems due to rock fracturing and the availability of feeding groundwaters. Wang and Manga (2015) and Sato et al. (2020) reported detailed descriptions of the opening or re-opening phases of ephemeral or permanent warm water springs related to significant local seismic events. According to Tamburello et al. (2022) thermal springs belonging to hydrothermal circuits are chiefly located in extensional faulted areas characterized by the occurrence of earthquakes above magnitude 4. Faults are characterized, among other parameters, by a length and by a width usually obtained by aftershock distribution (Wells and Coppersmith, 1994). In turn, length and width are roughly proportional to the magnitude of mainshocks capable of inducing faulting effects (Leonard, 2010). Seismic events below magnitude 4 are generally considered not to have sufficient energy to generate highly faulted areas, and/or faults of sufficient length and width to sustain hydrothermal circulation (Wells and Coppersmith, 1994). On the reverse, earthquakes in the magnitude range of 4–6 are believed to generate fault lengths in the range of 1–30 km (Wells and Coppersmith, 1994). Most earthquakes occur in the crust, in the depth range of 10–40 km (e.g., Maggi et al., 2000), which implies that earthquakes below magnitude 6 do not have the energy to generate faults capable of deepening from the surface down to the bottom of the Earth's crust. Conversely, moderate and strong seismic events (M>6.5) can maintain relatively high values of crustal permeability during geological time allowing for the emission of mantle-derived geofluids (Figure 1). Faulting induced by seismic events of the considered catalog has been effective in generating thermal springs emissions belonging to hydrothermal systems due to rock fracturing and the availability of feeding groundwaters. In order to better understand the effects of tectonic and possible geothermal anomalies on thermal spring distribution the heat flow map compiled by Lucazeau (2019) has been considered (Figure 1). Thermal springs appear mostly related to seismic activity that occurred in areas characterized by relatively recent (0.2 Ma) orogenetic phases (Hasterok et al., 2022) while a further group of thermal springs is located in areas not affected by volcanic activity or by significant seismic activity. In these areas, possible effects of palaeotectonic activity belonging to orogenetic phases of the first Quaternary period (1–2 Ma) (Hasterok et al., 2022) probably survived during geological time. This is the case in Brazil.

3.2 Helium, geodynamic, and seismicity

Noble gases and He isotope ratios in particular, can be used as effective tools (e.g., Mamyrin and Tolstikhin, 1984; Porcelli et al., 2002; Ozima and Podosek, 2004; Burnard, 2013; Sano et al., 2014; Sano et al., 2015; Liu et al., 2023) to study the origin of deep (crustal or mantle) degassing in active tectonic regions, and are deemed capable of providing information on the presence of faults of considerable extension and depth produced by recent and past M>6 earthquakes. Figure 2 shows the R/Ra values for all the helium isotope data available in Abedini et al. (2006) and updated in this work, with respect to the earthquake distribution deduced from the databases described by Storchak et al. (2013); http://www.isc.ac.uk/iscgem/ accessed on 20 July 2023) and with respect to volcanic edifice distribution (Hasterok et al., 2022 and references therein).

We consider the highest $^3He/^4He$ value as representative of the region of provenance when multiple analyses are available. Where available, the $^3He/^4He$ values normalized to air and corrected for air contamination (R_C) are preferred to air-normalized values (R_A), to exclude helium isotope data possibly affected by the entrainment of air-derived helium (e.g., Craig et al., 1978; $R_A = (^3He/^4He)_m/(^3He/^4He)_{air}$). Typical crustal values are about 0.02 R_A, due to relatively high ^4He continental abundances generated via $U-Th$ decay (e.g., Mamyrin and Tolstikhin, 1984; Andrews, 1985). Mantle values are 6–8 R_A for the old subcontinental lithospheric mantle (SCLM) and mid-ocean ridge basalts (MORB), respectively (e.g., Kurz et al., 1982; Dunai and Baur, 1995; Gautheron and Moreira, 2002). Taking these end-members as reference, we tentatively consider a threshold of $R_C > 1.22\,R_A$ to clearly identify geofluids with a high mantle component. The $R_C = 1.22\,R_A$ value corresponds to a mantle contribution of 15% (MORB) to 20% (SLCM), depending on the geotectonic environment. An even higher contribution of about 22.3% can be estimated in subduction zones, where the mantle component is characterized by an average value of 5.4 ± 1.9 R_A (e.g., Hilton et al., 2002). Interestingly, a different threshold than the relatively conservative value of $R_C > 1.22\,R_A$ selected here could be used to trace unequivocally mantle contribution in surficial fluids. For example, a threshold value of 1 R_A would indicate the presence of a magmatic or mantle helium contribution of up to 12.3%, based on a MORB-type signature of the local mantle component, in the case where atmospheric contamination and/or contribution may be waived based on checking of $^4He/^{20}Ne$ values (e.g., Craig et al., 1978). In the absence of information on $^4He/^{20}Ne$, in our analysis we adopted the conservative approach of considering only $^3He/^4He$ significantly higher than the atmospheric ratio ($> 1.22\,R_A$).

Most frequent values (about 43% of the considered database) are below the threshold of 1.22 Ra. The highest values are found close to volcanic areas, in rifted geological environments, and in anomalously high heat flow areas, with maxima recorded in Iceland (e.g., Hilton et al., 1990; Poreda et al., 1992), where a mantle plume reaches the earth's surface.

One of the primary objectives of seismology is to accurately delineate and analyze the diverse physical characteristics of the Earth, including but not limited to temperature, composition, volatile content, and the existence of partial melt. Over the past 2 decades, there has been a significant enhancement in the resolution of global S wave upper mantle tomographic models. The primary factor contributing to this phenomenon is the expansion of accessible data and the advancement of automated methodologies capable of analyzing a substantial volume of surface wave seismograms. In particular, Lebedev and van der Hilst (2008) observed that low-Sv-velocity anomalies beneath mid-ocean ridges extend down to ~100 km depth. Pronounced seismic lithosphere beneath cratons extends down to ~200 km. Low-velocity zones are weak or absent beneath most cratons. Debayle et al. (2016 and references therein) discovered a notable azimuthal anisotropy inside

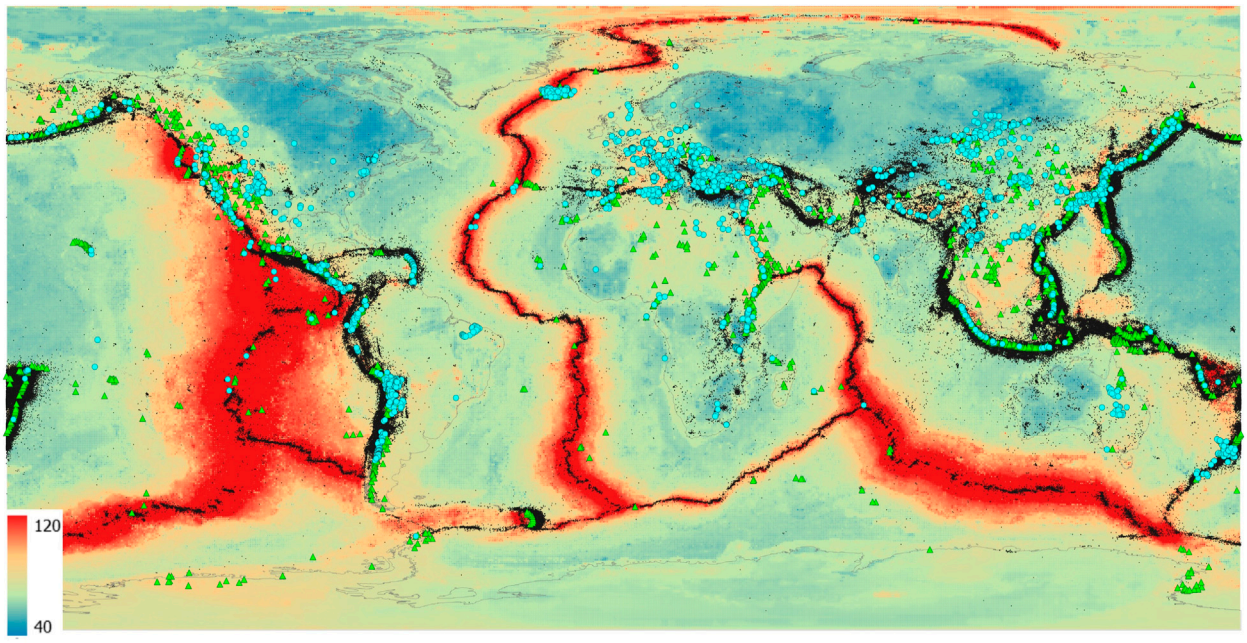

FIGURE 2
Heat flow map (Lucazeau, 2019) with location of (1) geofluids analyzed for helium isotope composition (blue dots; Abedini et al., 2006; revised and updated), (2) Holocenic and Pleistocenic volcanoes (green triangles; Global Volcanism Program, 2013), (3) 4<M<9.2 earthquakes (black dots; Storchak et al., 2013; http://www.isc.ac.uk/iscgem/ accessed on 20 July 2023).

the first 200 km of the Earth's mantle. Importantly, their findings indicate that this anisotropy does not exhibit a greater extent beneath continents compared to oceans. In their study, Adenis et al. (2017) presented also a comprehensive model of shear wave attenuation in the upper mantle on a global scale. The findings of their research demonstrate a notable association between surface tectonics and shear wave attenuation, specifically up to a depth of 200 km. The model reveals that regions underlying continents exhibit lower levels of attenuation, whilst regions underlying oceans display higher levels of attenuation. Anomalies that exhibit attenuation are observed beneath mid-ocean ridges at depths reaching 150 km, as well as beneath the majority of Pacific hot spots spanning from the lithosphere to the transition zone. The existence of extensive attenuating anomalies observed at a depth of 150 km in the Pacific Ocean indicates the presence of many thermal plumes situated within the asthenosphere. Montagner et al. (2007) provided pieces of evidence to support the existence of a direct correlation between the inferred mantle depth origin based on seismic tomography and the $^{3}He/^{4}He$ ratios observed in erupted magmas on a continental scale. The utilization of surface wave dispersion measurements and seismic tomography has provided insights into the relationship between tectonic settings and lithospheric seismic velocities. It has been observed that old cratons exhibit the highest seismic velocities, whereas tectonically active places tend to have relatively lower velocities. These findings could be better constrained by $^{3}He/^{4}He$ data and by heat flux data.

Considering the dispersion of S-waves (Debayle et al., 2016; Hasterok et al., 2022; see Figure 4), it was observed that most of anomalous ^{3}He areas are located above rock volumes affected by significantly low Vs. values.

Low Vs. values at depths in the order of 70 km are routinely interpreted as areas where partial melting processes are active (the phenomenon that occurs when a rock is subjected to temperatures high enough to cause certain minerals to melt, but not all of them). Therefore, under such conditions, the presence of fluids cannot be excluded, actually, it is very likely. S-wave dispersion may indicate, among others, the occurrence of deep-seated geofluids (Shito et al., 2006; Anderson, 2007; Unsworth and Rondenay, 2013). The obtained map of Helium 3 values has been compared with earthquake distribution deduced by databases described by Storchak et al. (2013); http://www.isc.ac.uk/iscgem/ accessed on 20 July 2023). High ^{3}He values recorded in high heat flow areas affected by deep geofluid feeding may be considered within tectonically active areas considered by the scientific literature currently available (e.g., Torgersen, 1993; Ballentine and Burnard, 2002; Polyak et al., 2020).

4 Selected candidate areas prone to significant next earthquakes

Figure 3 shows the correlation between heat flow and S-wave negative velocity perturbations for those areas where non-volcanic geofluids issue at the surface. In particular, this diagram only includes geofluids with an approximate minimum mantle contribution of 15%, as indicated by their $^{3}He/^{4}He > 1.22$ Ra. The top-left corner of Figure 4 shows regions characterized by relatively high heat flow values (Lucazeau, 2019) that are significantly affected by negative velocity perturbations (Debayle et al., 2016; Hasterok et al., 2022). This feature is typically associated with regions of major degassing, possibly linked to hidden magmatic bodies, or mantle

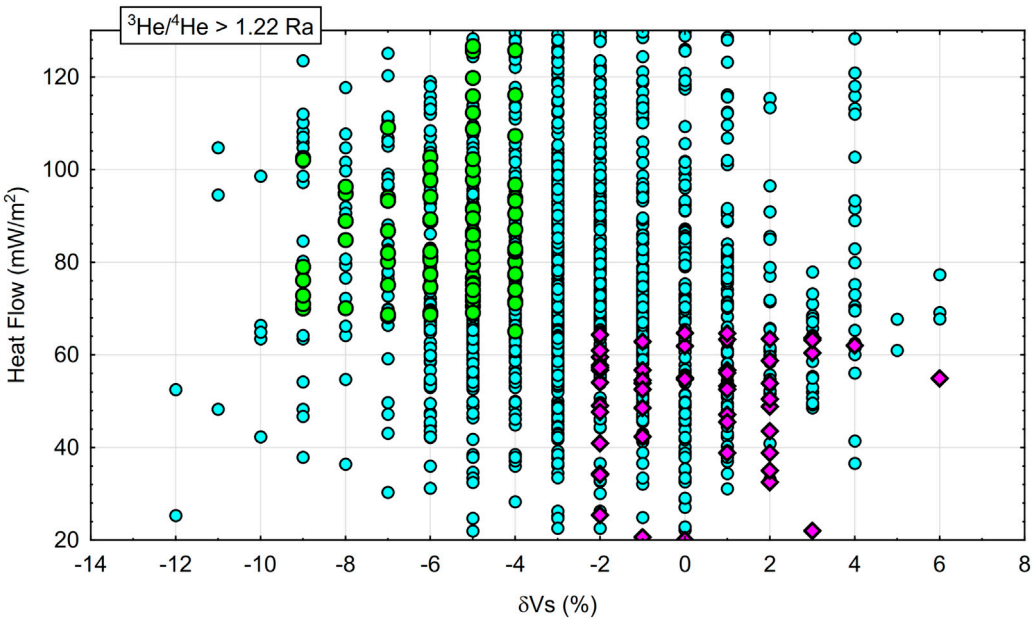

FIGURE 3
Heat flow vs. δVs (%) correlation plot for non-volcanic geofluids with $^3He/^4He$ > 1.22 Ra (after Abedini et al., 2006, modified and updated). Within this framework, we consider as "non-volcanic" those geofluids that emerge at the Earth surface at a minimum distance of 30 km from main volcanic edifices (see text). Green dots: geofluids collected in high heat flow areas (Lucazeau, 2019), characterized by negative δVs (%) perturbations (Debayle et al., 2016; Hasterok et al., 2022). Purple diamonds: geofluids collected in low heat flow areas (i.e., heat flow below the average value of continental areas; Lucazeau, 2019), scarcely or unaffected by negative δVs (%) perturbations (Debayle et al., 2016; Hasterok et al., 2022).

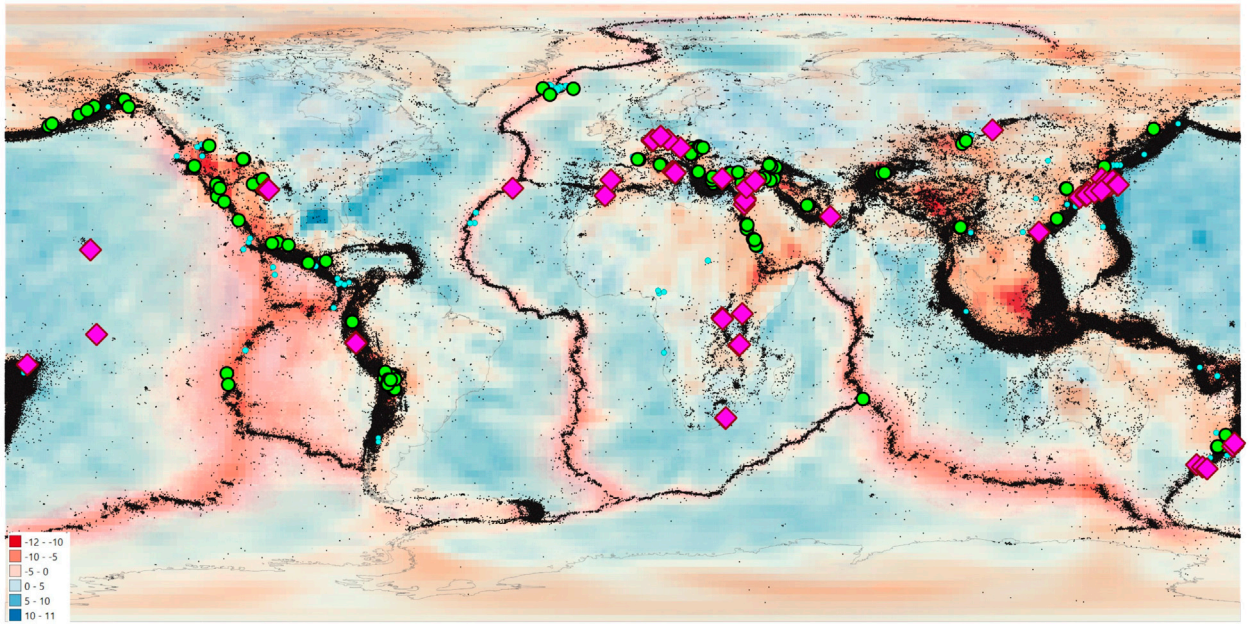

FIGURE 4
S-wave Dispersion map (Debayle et al., 2016; Hasterok et al., 2022) with location of non-volcanic fluid emissions (i.e., minimum distance of 30 km from main volcanic edifices, see text) characterized by R >1.22 Ra. Green dots: high heat flow areas (Lucazeau, 2019), significantly affected by negative δVs (%) values (Debayle et al., 2016; Hasterok et al., 2022). Purple diamonds: low heat flow areas (Lucazeau, 2019) scarcely affected, or unaffected, by significant δVs (%) values (Debayle et al., 2016; Hasterok et al., 2022). Black dots - 4<M<9.2 earthquakes (Storchak et al., 2013; http://www.isc.ac.uk/iscgem/ accessed on 20 July 2023).

plumes capable of conveying mantle fluids up to the surface, as occurs in Iceland (e.g., Samuel and Farnetani, 2003; Jackson et al., 2017). The low-right portion of the graph contains representative points from areas characterized by heat flow values below the average continental value (Lucazeau, 2019), which are scarcely affected, or unaffected, by significant S-wave negative velocity perturbations (Debayle et al., 2016; Hasterok et al., 2022 – see also Supplementary Figure S1). The latter areas, albeit apparently not always affected by frequent recent earthquakes recorded in seismic catalogs, have probably been affected by tectonic activities in the past capable of inducing faulting processes which reach the mantle or the lower crust like seismic events characterized by $M \geq 6.5$.

In areas identified by purple diamonds (Figure 4) and characterized by seismicity values that often do not coincide with the maximum magnitude values recorded in the world, relatively low heat flow, lack of close volcanic edifices, non-significant S-wave negative velocity perturbations values, possible deep-rooted faults, did not close during the geological time and were poorly affected by self-sealing phenomena, thus revealing possible still active tectonic strains capable of increasing crustal permeability, as observed by other authors in selected areas where noble gas prospections were carried out for different research purposes (e.g., Italiano et al., 2000; Italiano et al., 2001; Caracausi and Sulli, 2019; Caracausi et al., 2022; Liu et al., 2023).

These findings allow us to not exclude, in principle, the possible occurrence of any future strong seismic events in the identified faulted areas due to the eventual long recurrence time of seismic events. Further unexpected areas could be in similar conditions, because the current, preliminary version of the graph, is capable of identifying only the most relevant end-members.

Further to this, because the here considered databases could be inherently incomplete, we cannot exclude that other regions around the world in addition to those identified in this manuscript are in similar conditions Supplementary Figure S2. An obvious outcome of this work is the recommendation to test the method again as soon as new and more extensive data are available.

5 Conclusion

Areas affected by significant tectonic activity have been identified by the mapping of thermal springs. In principle, all the areas where significant tectonic activity is superimposed upon areas that host thermal springs should continue over time to host seismic events until large-scale geodynamic events modify present-day global tectonic activity. Anomalous geofluid locations emitting mantle-derived significant components have been found also outside of known seismically active areas, particularly in areas affected by anomalous heat flow and by the possibly anomalous dispersion of S wave values. After excluding the existence of magma-related local geological disturbances, the identified mantle-derived geofluid emissions could be affected, in principle, by moderate and strong seismic events (M>6) which maintained relatively high crustal permeability values during geological time, in spite of the lack of a relatively high frequency of earthquakes in catalogs which consider only the last 6 decades, the lack of volcanic vents, the lack of anomalous heat flow and the lack of enhanced values of negative S wave perturbation. The existence of geofluid emissions in the form of thermal springs shows that there is a first quantum value in crustal permeability, and is determined by the occurrence of seismic events characterized by magnitude values of 4 ± 0.5 and 6 ± 0.5. There is also a second quantum value in the crustal permeability evidenced by a significant presence of Helium 3 in geofluids and is determined by the occurrence of seismic events characterized between 6 ± 0.5 and 9.2. The identified sites should be considered in pattern recognition studies that accompany NDSHA. In the recent past, flaws in seismic hazard evaluations have been reported by various Authors (Kossobokov and Nekrasova, 2012; Wyss et al., 2012, etc.). The incompleteness of seismic catalogs could be considered, among others, responsible for possible seismic hazard underevaluation in various sites on Earth. The identified procedures, in principle, could help to better identify areas in which deep faults capable of reaching the upper mantle layers permanently remain affected by increased values of crustal permeability, probably due to unrevealed or undetected slight crustal strain phenomena. We have set up a procedure to preliminarily identify potential earthquake-prone areas in unexpected sites of the world. The adopted procedures may be further improved by considering less conservative filters or by means of further sampling and analysis of local geofluids. Detailed site-by-site studies will better clarify the identified features of unexpected potentially tectonically active areas. Geofluids have been confirmed to be powerful tools capable of contributing to a better description of future seismic hazard evolutive trends. Recent Seismic Hazard Assessment methods take into account morpho-structural zoning, which in turn takes into account nodes (fractured areas), lineaments, and topographical features such as the highest and lowest elevations of the studied area. The present work added geofluids to the previously known list of geological parameters useful for Seismic Hazard Assessment.

Data availability statement

The databases used in this work for thermal waters, seismic events and selected superficial manifestations with He isotope signature R >1.22 Ra are available upon request from the corresponding author.

Author contributions

GM: Conceptualization, Methodology, Supervision, Writing–original draft. LP: Conceptualization, Data curation, Methodology, Visualization, Writing–review and editing. GF: Data curation, Software, Supervision, Validation, Writing–review and editing. FG: Conceptualization, Data curation, Investigation, Methodology, Supervision, Validation, Writing–review and editing.

Funding

The author(s) declare that no financial support was received for the research, authorship, and/or publication of this article.

Acknowledgments

The authors warmly acknowledge the two reviewers for their constructive criticisms, and P. Capuano for his editorial supervision.

GM carried out present research activity within the frame of project proposal IGCP-724, Fluid Geochemistry and Earthquake Forecasting. Part of present paper has been presented during AOGS 2023.

Conflict of interest

The authors declare that the research was conducted in the absence of any commercial or financial relationships that could be construed as a potential conflict of interest.

The author(s) declared that they were an editorial board member of Frontiers, at the time of submission. This had no impact on the peer review process and the final decision.

Publisher's note

Supplementary material

The Supplementary Material for this article can be found online at: https://www.frontiersin.org/articles/10.3389/feart.2023.1286817/full#supplementary-material

References

Abedini, A. A., Hurwitz, S., and Evans, W. C. (2006). *USGS-NoGaDat-A global dataset of noble gas concentrations and their isotopic ratios in volcanic systems (No. 202)*. Reston, Virginia: US Geological Survey.

Adenis, A., Debayle, E., and Ricard, Y. (2017). Attenuation tomography of the upper mantle. *Geophys. Res. Lett.* 44 (15), 7715–7724. doi:10.1002/2017gl073751

Anderson, D. L. (2007). *New theory of the earth*. Cambridge: Cambridge University Press, 384.

Andrews, J. N. (1985). The isotopic composition of radiogenic helium and its use to study groundwater movement in confined aquifers. *Chem. Geol.* 49 (1-3), 339–351. doi:10.1016/0009-2541(85)90166-4

Ballentine, C. J., and Burnard, P. G. (2002). Production, release and transport of noble gases in the continental crust. *Rev. Mineralogy Geochem.* 47 (1), 481–538. doi:10.2138/rmg.2002.47.12

Bredehoeft, J. D., and Norton, D. L. (1990). "Mass and energy transport in a deforming Earth's crust," in *The role of fluids in crustal processes* (Washington, D.C: National Academies Press), 27–41.

Brogi, A., Alçiçek, M. C., Liotta, D., Capezzuoli, E., Zucchi, M., and Matera, P. F. (2021). Step-over fault zones controlling geothermal fluid-flow and travertine formation (Denizli Basin, Turkey). *Geothermics* 89, 101941. doi:10.1016/j.geothermics.2020.101941

P. Burnard (Editor) (2013). *The noble gases as geochemical tracers* (Berlin Heidelberg: Springer). doi:10.1007/978-3-642-28836-4

Caracausi, A., Buttitta, D., Picozzi, M., Paternoster, M., and Stabile, T. A. (2022). Earthquakes control the impulsive nature of crustal helium degassing to the atmosphere. *Commun. Earth Environ.* 3, 224. doi:10.1038/s43247-022-00549-9

Caracausi, A., and Sulli, A. (2019). Outgassing of mantle volatiles in compressional tectonic regime away from volcanism: the role of continental delamination. *Geochem. Geophys. Geosyst.* 20, 2007–2020. doi:10.1029/2018gc008046

Chandrasekharam, D., Lashin, A., Al Arifi, N., Al Bassam, A. A., and Varun, C. (2015). Evolution of geothermal systems around the Red Sea. *Environ. Earth Sci.* 73, 4215–4236. doi:10.1007/s12665-014-3710-y

Chiodini, G., Cardellini, C., Di Luccio, F., Selva, J., Frondini, F., Caliro, S., et al. (2020). Correlation between tectonic CO2 Earth degassing and seismicity is revealed by a 10-year record in the Apennines, Italy. *Sci. Adv.* 6 (35), eabc2938. doi:10.1126/sciadv.abc2938

Ciezkowski, W., Gröning, M., Leśniak, P. M., Weise, S. M., and Zuber, A. (1992). Origin and age of thermal waters in Cieplice Spa, Sudeten, Poland, inferred from isotope, chemical and noble gas data. *J. Hydrology* 140 (1-4), 89–117. doi:10.1016/0022-1694(92)90236-o

Cornell, C. A. (1968). Engineering seismic risk analysis. *Bull. Seismol. Soc. Am.* 58, 1583–1606. doi:10.1785/bssa0580051583

Craig, H., Lupton, J. E., and Horibe, Y. (1978). "A mantle helium component in circum-Pacific volcanic gases: hakone, the Marianas, and Mt. Lassen," in *Terrestrial rare gases. 16*. Editors E. C. Alexander and M. Ozima (Tokyo: Center for Academic Press), 3.

Curewitz, D., and Karson, J. A. (1997). Structural settings of hydrothermal outflow: fracture permeability maintained by fault propagation and interaction. *J. Volcanol. Geotherm. Res.* 79, 149–168. doi:10.1016/S0377-0273(97)00027-9

D. Porcelli, R. Ballentine, and R. Wieler (Editors) (2002). *Noble gases in Geochemistry and cosmochemistry, vol. 47* (Washington DC: Mineralogical Society of America).

Debayle, E., Dubuffet, F., and Durand, S. (2016). An automatically updated S-wave model of the upper mantle and the depth extent of azimuthal anisotropy. *Geophys. Res. Lett.* 43, 674–682. doi:10.1002/2015gl067329

Dunai, T. J., and Baur, H. (1995). Helium, neon and argon systematics of the european subcontinental mantle:implications for its geochemical evolution. *Geochimica Cosmochimica Acta* 59, 2767–2783. doi:10.1016/0016-7037(95)00172-v

Gautheron, C., and Moreira, M. (2002). Helium signature of the subcontinental lithospheric mantle. *Earth Planet. Sci. Lett.* 199, 39–47. doi:10.1016/s0012-821x(02)00563-0

Gelfand, I. M., Guberman, S. A., Keilis-Borok, V. I., Knopoff, L., Press, F., Ranzman, I. Y., et al. (1976). Pattern recognition applied to earthquake epicenters in California. *Phys.Earth Planet. Inter.* 11, 227–283. doi:10.1016/0031-9201(76)90067-4

Giardini, D., Grünthal, G., Shedlock, K. M., and Zhang, P. (2003). "The GSHAP global seismic hazard map. In international," in *Handbook of earthquake and engineering seismology*. Editors W. Lee, H. Kanamori, P. Jennings, and C. Kisslinger (Amsterdam, Netherlands: Academic Press), 1233–1239.

Gleeson, T., and Ingebritsen, S. (2017). *Crustal permeability*. Chichester: Wiley-Blackwell. ISBN 9781119166566 p 451.

Gold, T., and Soter, S. (1984). Fluid ascent through the solid lithosphere and its relation to earthquakes. *Pure Appl. Geophys.* 122, 492–530. doi:10.1007/bf00874614

Gorshkov, A., and Soloviev, A. (2021). "Morphostructural zoning for identifying earthquake-prone areas," in *Earthquakes and sustainable infrastructure: neodeterministic (NDSHA) approach guarantees prevention rather than cure*. Editors G. F. Panza, V. G. Kossobokov, E. Laor, and B. De Vivo (Elsevier), 135–149.

Gorshkov, A. I., Kossoboko, V., and Soloviev, A. A. (2003). "Recognition of earthquake prone areas," in *Nonlinear dynamics of the lithosphere and earthquake prediction*. Editors V. Keilis-Bork, and A. A. Soloviev (Heidelberg: Springer), 235–320.

Graser, A. (2013). *Learning QGIS 2.0*. Birmingham: Packt Publishing.

Hasterok, D., Halpin, J. A., Collins, A. S., Hand, M., Kreemer, C., Gard, M. G., et al. (2022). New maps of global geological provinces and tectonic plates. *Earth-Science Rev.* 231, 104069. doi:10.1016/j.earscirev.2022.104069

Hilton, D. R., Fischer, T. P., and Marty, B. (2002). Noble gases and volatile recycling at subduction zones. *Rev. Mineralogy Geochem.* 47, 319–370. doi:10.2138/rmg.2002.47.9

Hilton, D. R., Grönvold, K., O'Nions, R. K., and Oxburgh, E. R. (1990). Regional distribution of 3He anomalies in the Icelandic crust. *Chem. Geol.* 88 (1-2), 53–67. doi:10.1016/0009-2541(90)90103-e

Irwin, W. P., and Barnes, I. (1980). Tectonic relations of carbon dioxide discharges and earthquakes. *J. Geophys. Res. Solid Earth* 85 (B6), 3115–3121. doi:10.1029/jb085ib06p03115

Italiano, F., Martelli, M., Martinelli, G., and Nuccio, P. M. (2000). Geochemical evidence of melt intrusions along lithospheric faults of the southern Apennines (Italy): geodynamic and seismogenic implications. *J. Geophys. Res.* 106, 13569–13578. doi:10.1029/2000jb900047

Italiano, F., Martinelli, G., and Nuccio, P. M. (2001). Anomalies of mantle-derived helium during the 1997–1998 seismic swarm of Umbria–Marche, Italy. *Geophys. Res. Lett.* 28, 839–842. doi:10.1029/2000gl012059

Jackson, M. G., Konter, J. G., and Becker, T. W. (2017). Primordial helium entrained by the hottest mantle plumes. *Nature* 542 (7641), 340–343. doi:10.1038/nature21023

Kossobokov, V. G., and Nekrasova, A. K. (2012). Global seismic hazard assessment Program maps are erroneous. *Seism. Instrum.* 48 (2), 162–170. doi:10.3103/s0747923912020065

Kramer, S. L. (1996). *Geotechnical earthquake engineering*. Pearson Education India. ISBN-10: 8131707180.

Krinitzsky, E. L. (1995). Deterministic versus probabilistic seismic hazard analysis for critical structures. *Eng. Geol.* 40, 1–7. doi:10.1016/0013-7952(95)00031-3

Kurz, M. D., Jenkins, W. J., and Hart, S. R. (1982). Helium isotopic systematics of oceanic islands and mantle heterogeneity. *Nature* 297, 43–47. doi:10.1038/297043a0

Kuz'mina, E. A., and Novopashina, A. V. (2018). Groundwater outflows and fault density spatial relation in the Baikal rift system (Russia). *Acque Sotterranee-Italian J. Groundw.* 7 (1). doi:10.7343/as-2018-317

Lahsen, A., Muñoz, N., and Parada, M. A. (2010). "Geothermal development in Chile," in Proceedings World Geothermal Congress (Vol. 25, p. 7), Bali, Indonesia, April 25-30, 2010.

Lebedev, S., and Van Der Hilst, R. D. (2008). Global upper-mantle tomography with the automated multimode inversion of surface and S-wave forms. *Geophys. J. Int.* 173 (2), 505–518. doi:10.1111/j.1365-246x.2008.03721.x

Leonard, M. (2010). Earthquake fault scaling: self-consistent relating of rupture length, width, average displacement, and moment release. *Bull. Seismol. Soc. Am.* 100, 1971–1988. doi:10.1785/0120090189

Liu, W., Zhang, M., Chen, B., Liu, Y., Cao, C., Xu, W., et al. (2023). Hydrothermal He and CO_2 degassing from a Y-shaped active fault system in eastern Tibetan Plateau with implications for seismogenic processes. *J. Hydrology* 620, 129482. doi:10.1016/j.jhydrol.2023.129482

Lucazeau, F. (2019). Analysis and mapping of an updated terrestrial heat flow data set. *Geochem. Geophys. Geosys.* 20, 4001–4024. doi:10.1029/2019gc008389

Lupton, J. E. (1983). TERRESTRIAL INERT GASES: isotope tracer studies and clues to primordial components in the mantle. *Ann. Rev. Earth Planet Sci.* 11, 371–414. doi:10.1146/annurev.ea.11.050183.002103

Maggi, A., Jackson, J. A., McKenzie, D., and Priestley, K. (2000). Earthquake focal depths, effective elastic thickness, and the strength of the continental lithosphere. *Geology* 28, 495–498. doi:10.1130/0091-7613(2000)28<495:efdeet>2.0.co;2

Manga, M., Beresnev, I., Brodsky, E. E., Elkhoury, J. E., Elsworth, D., Ingebritsen, S. E., et al. (2012). Changes in permeability caused by transient stresses: field observations, experiments, and mechanisms. *Rev. Geophys.* 50 (2). doi:10.1029/2011rg000382

Mason, B. G., Pyle, D. M., and Oppenheimer, C. (2004). The size and frequency of the largest explosive eruptions on Earth. *Bull. Volcanol.* 66 (8), 735–748. doi:10.1007/s00445-004-0355-9

Montagner, J. P., Marty, B., Stutzmann, E., Sicilia, D., Cara, M., Pik, R., et al. (2007). Mantle upwellings and convective instabilities revealed by seismic tomography and helium isotope geochemistry beneath eastern Africa. *Geophys. Res. Lett.* 34 (21), L21303. doi:10.1029/2007gl031098

O'nions, R. K., and Oxburgh, E. R. (1983). Heat and helium in the earth. *Nature* 306 (5942), 429–431. doi:10.1038/306429a0

Ozima, M., and Podosek, F. A. (2004). *Noble gas Geochemistry*. 2nd edition. Cambridge: Cambridge University Press, 286.

Panza, G. F., La Mura, C., Peresan, A., Romanelli, F., and Vaccari, F. (2012). Seismic hazard scenarios as preventive tools for a disaster resilient society. *Adv. Geophys.* 53, 93–165. Elsevier. doi:10.1016/B978-0-12-380938-4.00003-3

Pesce, A. H. (2005). "Argentina country update," in *Proceedings world geothermal congress 2005 antalya* (Turkey: International Geothermal Association).

Petersen, M. D., Zeng, Y., Haller, K. M., McCaffrey, R., Hammond, W. C., Bird, P., et al. (2014). *Geodesy- and geology-based slip rate models for the Western United States (excluding California) national seismic hazard maps*. Open-File Report 2013–1293. Reston, VA: U.S. Geological Survey, 80. doi:10.3133/ofr20131293

Polyak, B. G., Tolstikhin, I. N., and Khutorskoi, M. D. (2020). Ascending heat and mass flow in continental crust: on the problem of driving forces of tectogenesis. *Izvestiya, Phys. Solid Earth* 56 (4), 490–510. doi:10.1134/s1069351320030088

Poreda, R. J., Craig, H., Arnorsson, S., and Welhan, J. A. (1992). Helium isotopes in Icelandic geothermal systems: I. ^{3}He, gas chemistry, and ^{13}C relations. *Geochimica Cosmochimica Acta* 56 (12), 4221–4228. doi:10.1016/0016-7037(92)90262-h

Samuel, H., and Farnetani, C. G. (2003). Thermochemical convection and helium concentrations in mantle plumes. *Earth Planet. Sci. Lett.* 207 (1-4), 39–56. doi:10.1016/s0012-821x(02)01125-1

Sano, Y., Hara, T., Takahata, N., Kawagucci, S., Honda, M., Nishio, Y., et al. (2014). Helium anomalies suggest a fluid pathway from mantle to trench during the 2011 Tohoku-Oki earthquake. *Nat. Commun.* 5, 3084. doi:10.1038/ncomms4084

Sano, Y., Kagoshima, T., Takahata, N., Nishio, Y., Roulleau, E., Pinti, D. L., et al. (2015). Ten-year helium anomaly prior to the 2014 Mt Ontake eruption. *Sci. Rep.* 5, 13069. doi:10.1038/srep13069

Sato, T., Kazahaya, K., Matsumoto, N., and Takahashi, M. (2020). Deep groundwater discharge after the 2011 Mw 6.6 Iwaki earthquake, Japan. *Earth Planets Space* 72, 54. doi:10.1186/s40623-020-01181-7

Shito, A., Karato, S.-I., Matsukage, K. N., Nishihara, Y., Jacobse, S., and Van Der Lee, S. (2006). *Towards mapping the three-dimensional distribution of water in the upper mantle from velocity and attenuation tomography*. Washington D.C.: Geophysical Monograph-American Geophysical Union, 225–236.

Storchak, D. A., Di Giacomo, D., Bondár, I., Engdahl, E. R., Harris, J., Lee, W. H., et al. (2013). Public release of the ISC–GEM global instrumental earthquake catalogue (1900–2009). *Seismol. Res. Lett.* 845, 810–815. doi:10.1785/0220130034

Tamburello, G., Chiodini, G., Ciotoli, G., Procesi, M., Rouwet, D., Sandri, L., et al. (2022). Global thermal spring distribution and relationship to endogenous and exogenous factors. *Nat. Commun.* 13 (1), 6378. doi:10.1038/s41467-022-34115-w

Tamburello, G., Pondrelli, S., Chiodini, G., and Rouwet, D. (2018). Global-scale control of extensional tectonics on CO2 earth degassing. *Nat. Commun.* 9 (1), 4608. doi:10.1038/s41467-018-07087-z

Torgersen, T. (1993). Defining the role of magmatism in extensional tectonics: helium 3 fluxes in extensional basins. *J. Geophys. Res. Solid Earth* 98 (9), 16257–16269. doi:10.1029/93jb00891

Twiss, R. J., and Moores, E. M. (1997). *Structural geology*. 2nd Ed. San Francisco, 73 CA: Freeman and Company, 736.

Unsworth, M., and Rondenay, S. (2013). "Mapping the distribution of fluids in the crust and lithospheric mantle utilizing geophysical methods," in *Metasomatism and the chemical transformation of rock* (Berlin, Heidelberg: Springer), 535–598. doi:10.1007/978-3-642-28394-9_133-642-28394-9_13

Vannoli, P., Martinelli, G., and Valensise, G. (2021). The seismotectonic significance of geofluids in Italy. *Front. Earth Sci.* 9, 579390. doi:10.3389/feart.2021.579390

Wang, C.-Y., Liao, X., Wang, L.-P., Wang, C.-H., and Manga, M. (2016). Large earthquakes create vertical permeability by breaching aquitards. *Water Resour. Res.* 52, 5923–5937. doi:10.1002/2016WR018893

Wang, C.-Y., and Manga, M. (2015). New streams and springs after the 2014 Mw 6.0 South Napa earthquake. *Nat. Commun.* 6, 7597. doi:10.1038/ncomms8597

Wang, K. (2008). *The types, distribution and basic characteristics of geothermal areas in China*. Geothermal Training Programme: Lectures on Geothermal areas in China Lecture 1. Orkustofnun, Grensásvegur 9, Reports 2008 IS-108 Reykjavík, Iceland Number 7.

Waring, G. A. (1965). Thermal springs of the United States and other countries of the world - a Summary. *U. S. Geol. Surv. Prof. Pap.* 492, 383.

Wells, D. L., and Coppersmith, K. J. (1994). New empirical relationships among magnitude, rupture length, rupture width, rupture area, and surface displacement. *Bull. Seism. Soc. Am.* 84, 974–1002. doi:10.1785/BSSA0840040974

Wexsteen, P., Jaffé, F. C., and Mazor, E. (1988). Geochemistry of cold CO2-rich springs of the scuol-tarasp region, lower engadine, Swiss alps. *J. Hydrology* 104 (1-4), 77–92. doi:10.1016/0022-1694(88)90158-8

Wu, Y., Zhou, X., Zhuo, L., Guangbin, T., Ma, J., and Wang, Y. (2023). Structural controls of the northern Red River Fault Zone on the intensity of hydrothermal activity and distribution of hot springs in the Yunnan-Tibet geothermal belt. *Geothermics* 109, 102641. doi:10.1016/j.geothermics.2022.102641

Wyss, M., Nekraskova, A., and Kossobokov, V. (2012). Errors in expected human losses due to incorrect seismic hazard estimates. *Nat. Hazards* 62, 927–935. doi:10.1007/s11069-012-0125-5

Yousefi, H., Noorollahi, Y., Ehara, S., Itoi, R., Yousefi, A., Fujimitsu, Y., et al. (2010). Developing the geothermal resources map of Iran. *Geothermics* 39 (2), 140–151. doi:10.1016/j.geothermics.2009.11.001

Zhang, Y., Romanelli, F., Vaccari, F., Peresan, A., Jiang, C., Wu, Z., et al. (2021). Seismic hazard maps based on neo-deterministic seismic hazard assessment for China seismic experimental site and adjacent areas. *Eng. Geol.* 291, 106208. doi:10.1016/j.enggeo.2021.106208